

Isotope shift of the 2^3P-3^3D transition in helium

R. R. Freeman, P. F. Liao, R. Panock, and L. M. Humphrey

Bell Laboratories, Holmdel, New Jersey 07733

(Received 27 March 1980)

The isotope shift of the transition 2^3P-3^3D between ^3He and ^4He is measured to an accuracy of 3 parts in 10^3 using the technique of Doppler-free intermodulated fluorescence spectroscopy. The hyperfine structure of ^3He in the 2^3P and 3^3D states is fully resolved and is fit to a magnetic-interaction hyperfine Hamiltonian. After removing the hyperfine interaction and assuming no specific isotope shift in the 3^3D state, the measured isotope shift agrees with theoretical values when variational wave functions are used to compute the specific mass shift of the 2^3P term.

INTRODUCTION

The role of the nucleus in determining the energy levels of an atomic system is not restricted to the nuclear charge: the finite mass enters as an isotopically dependent term expressing the nuclear kinetic energy. This energy is given by $(\sum P_i)^2/2M$, where $\sum P_i$ is the sum of the individual electron momenta and M is the nuclear mass. These terms in the kinetic energy $\sum P_i^2/2M$ yield a rigorous correction to the infinite mass energy of $M/(M+m)$, where m is the electron mass and M is the nuclear mass. This correction, which is independent of the orbital wave functions, is termed the "normal mass shift." Additional corrections arise from terms in the kinetic energy of the form $(\sum_{i \neq k} \vec{P}_i \cdot \vec{P}_k)/M$. These terms must be evaluated using calculated wave functions and give rise to the "specific mass shift."

In the case of helium, the specific mass effect plays a significant role in determining the total isotope shift. Since the electronic wave functions of helium can, in principle, be computed quite precisely, a measurement of the isotopic shift of transitions between ^3He and ^4He can provide an excellent test of the accuracy of computed wave functions. This is especially true for the lower lying terms, particularly P states, because the $(\vec{P}_1 \cdot \vec{P}_2)/M$ expectation value is quite sensitive to any configuration interactions in the computed wave functions. In this paper we present the results of measurement of the isotope shift of the 2^3P-3^3D transition between ^3He and ^4He . The shift is measured to an accuracy of 3 parts in 10^3 and represents an improvement of approximately a factor of 10 in accuracy over previous determinations.

There have been several measurements of isotope shifts of transitions in the helium system,¹ but the standard work is recognized to be by Fred, Tomkins, Brody, and Hamermesh,² who measured the isotope shift between ^3He and ^4He on some 31 transitions observed in emission. Specifically,

they measured the isotope shift of the $\lambda = 587.5$ nm 2^3P-3^3D transition as -3690 ± 210 MHz, where the assigned uncertainty arises from the average of multiple-interferometer ring diameter measurements. Because the Doppler width obscured the majority of the hyperfine components on this transition in ^3He , the contribution of the hyperfine interaction in ^3He to the apparent isotope shift was calculated *ab initio*, and calculated center-of-gravity positions were used to determine the true isotope shift.

In our measurements, we employed a Doppler-free laser saturation technique that allowed the resolution of the majority of the hyperfine structure of the 2^3P-3^3D transition in ^3He and resolution of the fine structure of ^4He . Enough of the individual hyperfine components were resolved that a complete determination³ of the hyperfine interaction in the 2^3P and 3^3D states in terms of a magnetic-interaction Hamiltonian was possible. Thus we were able to remove the contribution of the hyperfine interaction to the apparent isotope shift quite precisely.

MEASUREMENT

We obtained Doppler-free laser spectra of the 587.5-nm (2^3P-3^3D) transition in ^3He and ^4He using the technique of intermodulated fluorescence spectroscopy.⁴ A pure helium (both isotopes) discharge with current densities of approximately 70 mA/cm² was operated in a 10-cm long, 3-mm bore diameter pyrex tube with a total pressure of 0.8 Torr. The tube voltage was 800 V. The laser radiation, obtained from a commercial tunable dye laser (Coherent 599), was split into two beams of approximately equal intensity: one beam was chopped at 900 Hz, while the other chopped at 570 Hz. The beams propagated in opposing directions through the tube perpendicular to the photomultiplier. The component of the fluorescence at 587.5 nm with a

beat frequency at 330 Hz was detected synchronously with the difference signal generated electronically from the two choppers. We also used the same configuration to detect the signal by monitoring the optogalvanic change in tube voltage⁵; however, we found that the fluorescence detection yielded, in general, a greater signal-to-noise ratio for a given averaging period.

The frequency intervals were determined by monitoring the transmission of part of the laser beam through a 1.225-meter interferometer. The interferometer was evacuated and temperature stabilized at 0°C. The free spectral range (FSR) was checked by measuring the $J=1-2$ separation⁶ in the 3^3D state of ^4He .

In Fig. 1 we show a low-resolution, wide-frequency sweep encompassing all fine and hyperfine transitions at $\lambda=587.4$ nm in ^3He and ^4He . The spectrum divides into roughly two regions: transitions originating from the 2^3P_0 ($F=\frac{1}{2}$) state and transitions originating from the $2^3P_{1,2}$ ($F=\frac{1}{2}, \frac{3}{2}, \frac{5}{2}$) states. These two regions are separated by approximately 1 cm^{-1} ; no attempt to measure this separation precisely was made. Rather, we used the well-known⁶ fine-structure intervals in 2^3P and 3^3D together with the observed ^4He transitions to measure accurately the relative frequency of the hyperfine components of ^3He for the two regions.

As is usually the case in saturation spectroscopy, the spectrum contains a large number of crossover resonances. These resonances are extremely useful in identifying the transitions, since they fall exactly halfway between true resonances which share either a common ground or excited state. Because the strength of the crossover signal depends upon (approximately) the geometric mean of the intensities of the participating transitions, the positions of crossover resonances also often allow the location of otherwise very weak true

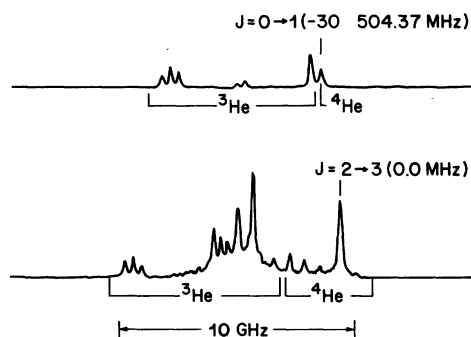


FIG. 1. Two laser scans showing Doppler-free intermodulated fluorescence resonances of ^3He and ^4He at $\lambda=587.5$ nm. The $2^3P_0-3^3D_1$ resonance of ^4He is located 30 504.37 MHz lower than the frequency of the $2^3P_2-3^3D_3$ resonance of ^4He .

resonances.

In Fig. 2 we show a recording of the fine-structure components ($2^3P_{1,2}-3^3D_{1,2,3}$) of ^4He . Also shown is a simultaneous recording of the transmission of the interferometer. The interval between the $2^3P_1-3^3D_2$ and $2^3P_1-3^3D_1$ resonances is used together with the known⁶ $J=2-3$ separation in 3^3D state to check the FSR calibration of the interferometer obtained from a measurement of its physical length. The transition $2^3P_2-3^3D_1$ is too weak to observe, yet the positive crossover signal with the $2^3P_2-3^3D_3$ signal is clearly visible. The transitions $2^3P_2-3^3D_3$ and $2^3P_2-3^3D_2$ are within 75 MHz of each other and are unresolvable; in addition, the predicted ratio of transition moments of $J=2-J=3$ compared to $J=2-J=2$ indicates that the observed resonance is due essentially to $2^3P_2-3^3D_3$ only. This figure also shows the weaker negative crossover signal arising from the shared 3^3D_2 excited state. The recorded linewidths of 100 MHz are presumably due primarily to broadening by free electrons in the plasma; increases in the helium pressure produced further broadening at a rate of only 35 ± 10 MHz/Torr. The observed fine and hyperfine splittings were found to be independent of pressure up to the maximum pressure employed, 3.5 Torr. Since, in general, the absolute shift of transitions by plasma interactions is on the order of 1/10 the plasma broadening,⁷ we feel our measurements accurately reflect the fine and hyperfine structure of an isolated helium atom.

We chose to operate the experiment in a weakly saturated regime in order to enhance the signal-to-noise ratio on the weaker transitions. The trade-off was an intensity dependent increase in

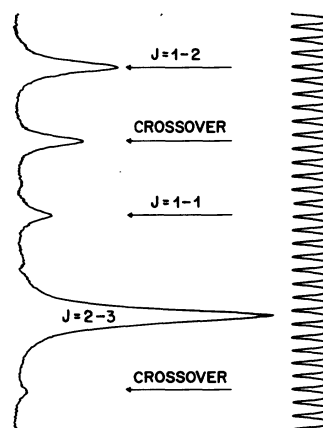


FIG. 2. Doppler-free intermodulated fluorescence spectrum containing transitions $2^3P_{1,2}-3^3D_{1,2,3}$ of ^4He . Also shown is the transmission of the 1.225-meter reference interferometer. The peaks are separated by 122.4 MHz.

linewidth. For the chosen intensity, 200 W/cm², the power broadening contribution to the linewidth was approximately 20 MHz; however, changes in laser intensity by a factor of 4 did not modify the observed splittings.

Figure 3 shows a schematic of the fine and hyperfine structure for the $\lambda = 587.5$ nm transition in the ⁴He-³He system. Since the hyperfine interaction in the $2^3P_{1,2}$ and $3^3D_{1,2,3}$ states dominates the fine structure in these states, $\vec{J}(=\vec{L}+\vec{S})$ is not a conserved quantity in ³He. Any calculation of the fine and hyperfine splittings in ³He must treat these perturbations on equal footing. The values of the splittings shown in Fig. 3 are the results of this measurement and analysis; in practice, the identification of the transitions started with theoretical splittings as given by Fred *et al.*², and corrections and/or reassignments were made in accordance with the data.

In Fig. 4 we show a portion of the hyperfine splittings of the $2^3P_{1,2} - 3^3D_{1,2,3}$ $\lambda = 587.5$ nm transition for ³He in which we have identified the transitions as $(2^3P_J)F - (3^3D_J)F'$. Also shown is the $J=1-2$ transition in ⁴He; the computed relative transition strengths, as discussed below, are also plotted at the frequency separations as calculated in this analysis.

Figure 5 shows a portion of the spectrum in which a transition in ³He lies closely spaced in frequency to a transition in ⁴He. This fortuitous placement allows a convenient measure of relative

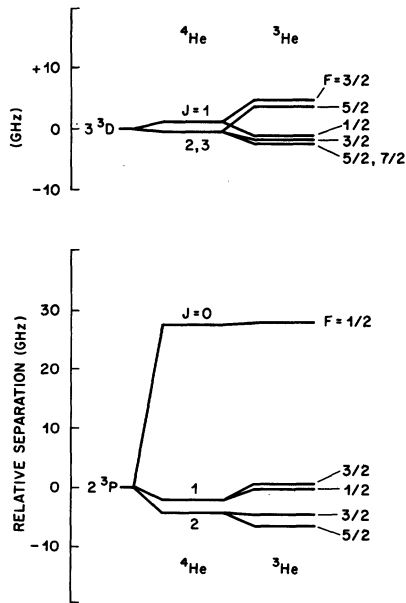


FIG. 3. Schematic diagram of the 3^3D and 2^3P energy states of ³He and ⁴He.

pressure shifts with increasing pressure. Fred *et al.*² reported an anonymously large differential pressure shift for the two isotopes for $\lambda = 587.5$ nm; our measurements indicate that each isotopic transition broadens at a rate of 35 ± 10 MHz/Torr⁸ and shifts to shorter wavelength at a rate of 4.6 ± 2 MHz/Torr. No significant difference in pressure shift or broadening for the two isotope components was found.

Analysis

The isotope effect refers to shifts in the term values of spinless electron energy levels; thus, to extract the term value changes from the observed spectrum, the contribution of the fine and hyperfine interactions to the observed energy must be removed. We have used a magnetic-interaction Hamiltonian to describe the fine and hyperfine interactions. We write the total Hamiltonian as

$$H = H_0 + H_{FS} + H_{HFS}, \quad (1)$$

where H_0 is the term value of the spinless electron and H_{FS} and H_{HFS} are the fine and hyperfine Hamiltonians, respectively. H_{FS} and H_{HFS} could, in principle, be calculated *ab initio*²; however, a much more reliably accurate method is to write the magnetic interactions in a parameterized form and to adjust the values of the parameters in such a way that the calculated splittings derived from the parameterized Hamiltonian have a minimum rms deviation from the observed splittings.

In our analysis we have assumed that the fine structure interactions in ³He are identical to those in ⁴He. The fine-structure Hamiltonian has its usual form for a two-electron atom⁹ and is parameterized as

$$H_{FS} = A\vec{L} \cdot \vec{S} + a\vec{L} \cdot \vec{K} + b \left(\frac{3(\vec{L} \cdot \vec{S})^2 + \frac{3}{2}(\vec{L} \cdot \vec{S}) - L^2S^2}{2S(2S-1)L(2L-1)} \right), \quad (2)$$

where $\vec{L} = \vec{L}_1 + \vec{L}_2$, $\vec{S} = \vec{S}_1 + \vec{S}_2$, and $\vec{K} = \vec{S}_1 - \vec{S}_2$. The hyperfine interaction for a two-electron atom is written⁹

$$H_{HFS} = \sum_{1,2} \left[2\mu_0\mu_n g_I r_i^{-3} [\vec{I} \cdot (\vec{r}_i \times \vec{P}_i) h^{-1}] + g_s g_I \mu_0 \mu_n \left(\frac{8}{3} \pi \right) \delta(r_i) \vec{S}_i \cdot \vec{I} + R\alpha^2 a_0^3 \left(\frac{m}{M} \right) r_i^{-3} \vec{I} \cdot \left(\vec{S}_i - \frac{3\vec{r}_i (\vec{r}_i \cdot \vec{S}_i)}{r_i^2} \right) \right], \quad (3)$$

where \vec{I} is the spin of the nucleus; $g_s \mu_0$ and $g_s \mu_n$ are the magnetic moments of the electron and nucleus, respectively; R is the Rydberg, α is the fine structure constant; a_0 is the Bohr radius, and

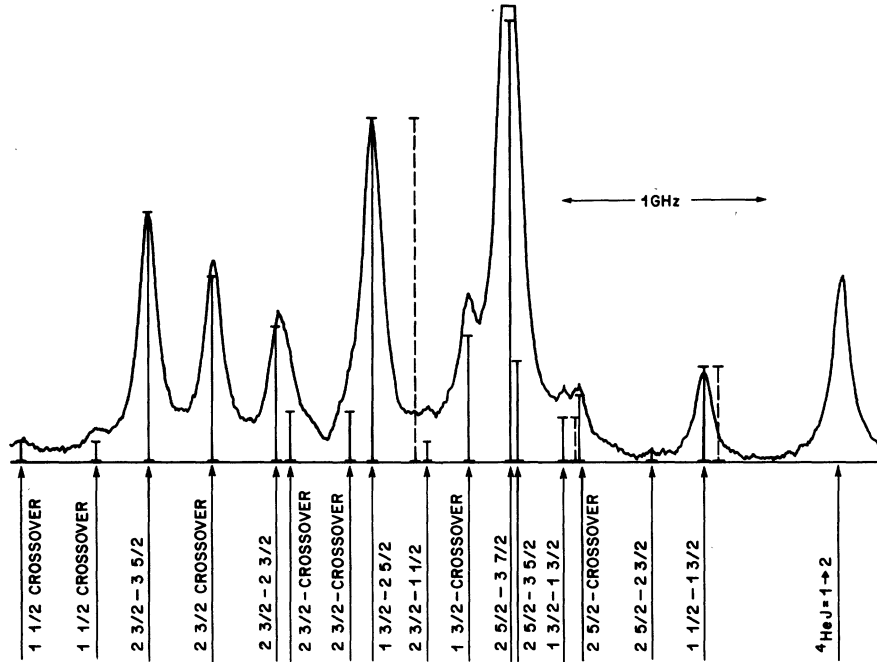


FIG. 4. Portion of Doppler-free intermodulated fluorescence spectrum containing $2^3P_{1,2}-3^3D_{1,2,3}$ transitions of ^3He and the $2^3P_1-3^3D_2$ transition of ^4He . The solid lines indicate predicted relative positions and intensities for the hyperfine transitions of ^3He which were obtained from a fit to the data. Dotted lines show predicted positions if singlet-triplet mixing is neglected.

m and M are the masses of the electron and nucleus, respectively. If one employs sums and differences of s_1 and s_2 , Eq. (3) may be written in its parameterized form as¹⁰

$$H_{\text{HFS}} = C\vec{I} \cdot \vec{L} + D\vec{I} \cdot \vec{\chi} + E\vec{I} \cdot \vec{S} + E\vec{I} \cdot \vec{K}. \quad (4)$$

Here, $\vec{\chi}$ is the vector formed from \vec{S} and $C^{(2)}[C^{(2)} = (\frac{4}{3}\pi)^{1/2}Y^{(2)}(\theta, \phi)]$. Note that the coefficient involving $\vec{I} \cdot \vec{S}$ is identical to $\vec{I} \cdot \vec{K}$ because for the 2^3P and 3^3D states the Fermi contact term arises from the inner $1s$ electron only.

Terms involving \vec{K} have matrix elements connecting singlet to triplet configurations of the same \vec{L} ; these terms do not contribute to splittings with-

in a given configuration. Similarly, terms in \vec{S} do not connect singlet to triplet, yet they contribute directly to splittings in the triplet states.

For the 2^3P state,⁹ $A = -5890.8$ MHz, $a = 639$ MHz, and $b = 6326.9$ MHz. For the 3^3D state,⁹ $A = -216.4$ MHz, $a = 267$ MHz, and $b = 509.6$ MHz. These parameters scale approximately as $\langle r^{-3} \rangle$ so that their n, l dependence is roughly $n^{-3}l^{-3}$. The hyperfine parameters C and D also scale as $\langle r^{-3} \rangle$; however, the parameter E is essentially independent of the orbital of the outer electron and thus constant for all $l s n l$ ($l > 0$) configurations of the atom.¹¹ For large enough n and l , the splittings in the triplet state will be dominated by the parameter E . This is in marked contrast to one electron-like spectra in which both the fine and hyperfine structure decrease rapidly with increasing n .

A consequence of the n independence of E is that the term $E\vec{I} \cdot \vec{K}$ is increasingly effective in coupling singlet and triplet levels as n increases because the energy separation of singlet-triplet terms decreases as n^{-3} . In this measurement the 3^3D state is mixed with the 3^1D state, which is removed by 102.36 GHz.⁹ Several strong perturbations of hyperfine levels in the 3^3D state are observed.³ The mixing of the 2^3P with the 2^1P is negligible due to the large energy separation.⁶

The matrix elements of Eqs. (3) and (4) were computed for the triplet $2P$ state and for both the

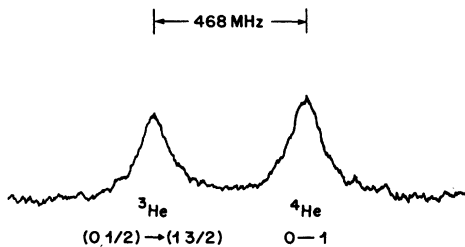


FIG. 5. Portion of Doppler-free intermodulated fluorescence spectrum containing $2^3P_0(F=\frac{1}{2})-3^3D_1(F=\frac{3}{2})$ transition of ^3He and the $2^3P_0-3^3D_1$ transition of ^4He . Total gas pressure in the discharge was approximately 0.9 Torr with a $^3\text{He}-^4\text{He}$ mixture of approximately 2:1.

triplet and singlet $3D$ states in an uncoupled $(S m_S, L m_L, M_L)$ basis for $M_F = M_S + M_L + M_L = \frac{1}{2}$. The resulting 5×5 (for the P state) or 8×8 (for the D state) matrices were diagonalized numerically by computer. Using the fine-structure values for ^4He , and an estimate for E obtained from Fred *et al.*², a prediction of the relative frequencies for the $(2^3P_J)F - (3^3D_J)F'$ transitions was made. From this prediction we were able to assign the probable labeling to the observed transitions.

The determination of the best choice of hyperfine constants C , D , and E for the 2^3P and 3^3D states was accomplished using standard, nonlinear least-squares regression routines.¹² The results have been presented earlier³; however, for completeness, they are also given in Table I. The errors are a combination of statistical uncertainties in the least-squares fitting and our estimation of the systematic experimental errors. The observed splittings in both the 3^3P and 3^3D states are predicted with the coefficients of Table I within an average rms deviation of 6 MHz, with no deviation exceeding 10 MHz. Given the experimental linewidths of 110 MHz and an average signal-to-noise ratio of approximately 15–20, we feel the parameterized Hamiltonian adequately describes the hyperfine perturbations.

Another measure of the correct choice of hyperfine constants is the predicted relative intensities compared to the experimental results. We calculated the relative intensities in the following manner. From the computer diagonalization we necessarily computed the eigenvectors in terms of the uncoupled basis set for each eigenenergy as well. From this eigenvector matrix the relative $\Delta M_F = 0$ transition moments for the $M_F = \frac{1}{2}$ transitions were immediately calculable. Employing the Wigner-Eckhart factorization,¹³ the ratio of $\Delta M_F = 0$ transition moments for the $M_F = \frac{1}{2}$ group to the $M_F = \frac{1}{2}, \frac{3}{2}, \frac{5}{2}$ groups could be readily calculated as ratios of the appropriate $3-j$ symbols.¹⁴ In this way the contributions of the various $(2F+1)M_F$ groups in a $(2^3P)F - (3^3D)F'$ transition could be correctly summed.

In Fig. 4 the relative transition moments for the observed transitions are plotted at their cal-

TABLE I. $H_{\text{HFS}} = C\vec{I} \cdot \vec{L} + D\vec{I} \cdot \vec{\chi} + E\vec{I} \cdot \vec{S} + E\vec{I} \cdot \vec{K}$.

	(2^3P) (\pm MHz)	(3^3D) (\pm MHz)
C	-39(15)	5(3)
D	+15(9)	0(5)
E	-4285(20)	-4325(10)
	4 transitions	5 transitions

culated relative frequency positions. Since we operated the experiment in a weakly saturated regime, we have calculated the relative transition strengths as proportional to the square of the relative dipole matrix elements. The dotted lines show the predicted positions of three components if singlet-triplet mixing in the 3^3D states is not included. The crossover strengths were calculated assuming that their intensities are given by the geometric mean of the intensities of the transitions involved.

The results of this analysis are summarized in Table II, where the energies of the components of the 2^3P and 3^3D states are shown relative to H_0 , the term value for the spinless electron in the $2P$ and $3D$ states. The isotope shift can now be read directly from the data by comparing any transition in ^3He to any transition in ^4He , using the fine and hyperfine energy shifts of Table II.

One result of this analysis is a confirmation of the proposed measurement scheme suggested in Ref. 2 i.e., the transition $(2\frac{5}{2}) - (3\frac{7}{2})$ in ^3He is predicted to be identical to the $J=2 - J=3$ transition in ^4He within experimental error (if there were no isotope shift). We have chosen not to measure these two transitions due to unresolved structure involving these transitions in both the ^3He and ^4He data. We have used two transitions in ^3He that are free of any unresolved structure and lie

TABLE II. Fine and hyperfine contributions to energy levels of $2P$ and $3D$.^a

^3He	
2^3P	3^3D
Energy of $2P \equiv 0.0$ MHz	Energy of $3D \equiv 0.0$ MHz
$J F$	$J F$
$0 \frac{1}{2} = +27\,923.3$	$1 \frac{3}{2} = +4752.0$
$1 \frac{3}{2} = +499.6$	$2 \frac{5}{2} = +3830.8$
$1 \frac{1}{2} = -180.3$	$1 \frac{1}{2} = -1071.8$
$2 \frac{3}{2} = -4\,664.3$	$2 \frac{3}{2} = -1808.9$
$2 \frac{5}{2} = -6\,471.1$	$3 \frac{5}{2} = -2429.2$
	$3 \frac{7}{2} = -2463.2$

^4He	
2^3P	3^3D
Energy of $2P = 0.0$ MHz	Energy of $3D = 0.0$ MHz
J	J
$0 = +27\,598.85$	$1 = +1097.78$
$1 = -2\,017.82$	$2 = -230.59$
$2 = -4\,309.07$	$3 = -305.77$

^a Estimated uncertainties are ± 6 MHz for ^3He levels and ± 0.2 MHz for ^4He levels.

TABLE III. Measurement of isotope shift.

Transitions	Measured displacement (MHz)	Fine and hyperfine contribution ^a (MHz)	Derived isotope shift (MHz)
$(1-\frac{1}{2}) \rightarrow (1-\frac{3}{2})$ $J=1-2$	-667(5)	+3145(8)	-3812(15)
$(0-\frac{1}{2}) \rightarrow (1-\frac{3}{2})$ $J=0-1$	-468(8)	+3330(8)	-3798(15)

^a See Table II.

close in frequency to completely resolved transitions in ^4He . These transitions are $(1-\frac{1}{2})-(1-\frac{3}{2})$ compared to $J=1-2$ (see Fig. 4) and $(0-\frac{1}{2})-(1-\frac{3}{2})$ compared to $J=0-1$ (see Fig. 5). The results of these measurements are given in Table III. Our best estimate for the isotope shift of the $\lambda=587.5$ nm 2^3P-3^3D transition in helium is $-3805(12)$ MHz, where the uncertainty reflects the errors in reducing the hyperfine contribution as well as errors in the direct measurement.

DISCUSSION

The largest contribution to the isotope shift comes from the reduced-mass correction known as the normal mass shift. This correction is determined only by the reduced masses of the isotopes and does not depend on the details of the electronic wave function. The normal mass shift in an energy level $\delta E_{\text{NMS}} = E - E_\infty$ for the two isotopes is

$$\delta E_{\text{NMS}}(^4\text{He}) = \frac{m}{M_4} T + 4 \frac{m}{m+M_4} R_\infty \quad (5)$$

$$\delta E_{\text{NMS}}(^3\text{He}) = \frac{m}{M_3} \left(\frac{m+M_4}{m+M_3} \right) T + 4 \frac{m}{m+M_3} R_\infty,$$

where T is the ionization energy of ^4He , M_4 and M_3 are the ^4He and ^3He nuclear masses, respectively, and R_∞ is the Rydberg constant (electron mass). The contributions of these shifts to the total isotope shift are listed in Table IV. The shifts in Eqs. (5) include a contribution due to the core of $[4m/(m+M)]R_\infty$; however, this contribution does not affect spectroscopic measurements, and hence the values for the normal mass shift in Table IV do not include this term.

The specific isotope effect is calculated as the expectation value of the perturbation term

$$-(\hbar^2/M) \vec{\nabla}_1 \cdot \vec{\nabla}_2, \quad (6)$$

and in first-order perturbation theory the energy change is given by¹⁵

TABLE IV. Calculated term value isotope shifts,*

Term	Normal ^a mass shift (MHz)	Hughes-Eckhart ^b	Refined specific ^b shift calculation (MHz)
		specific mass shift (MHz)	
2^3P	-39 270	+16 939	+19 034 ^c 19 050 ^d
3^3D	-16 406	0.0	

* Total term mass shift = normal shift + specific shift.

^a Derived number using term energies of Ref. 6 as discussed in the text.

^b See Ref. 2.

^c Ref. 19; derived by subtracting -39270 MHz from the total mass shift given in Ref. 19.

^d Ref. 20; this value was obtained by using tabulated values for the mass-polarization correction term, ϵ_M .

$$\Delta W = -(\hbar^2/M) \int \psi^* \vec{\nabla}_1 \cdot \vec{\nabla}_2 \psi d\vec{r}. \quad (7)$$

Hughes and Eckhart¹⁶ first evaluated Eq. (7) by taking ψ to be linear combinations of products of hydrogenic eigenfunctions. On this approximation, ΔW is zero for all even parity $l s n l$ configurations of the helium atom. For $1,^3P$ terms the specific mass effect may be written in terms of the effective nuclear charges "seen" by the two electrons.¹⁷

More exact wave functions have been calculated which take into account configuration interactions; these wavefunctions yield nonzero values for ΔW from Eq. (6) for states other than P states, especially S states.¹⁸ In addition, the more exact calculations give quite different results from the Hughes-Eckhart evaluation for the P states.^{19,20} In Table IV we show the calculated term value shifts for the 2^3P and 3^3D states. To our knowledge no precise wave functions have been calculated for the 3^3D states; the Hughes-Eckhart approximation yields zero shift for the 3^3D state.

The measured isotope shift of the $\lambda=587.5$ nm transition involves the isotope term values of both the 2^3P and 3^3D states. Therefore, a direct comparison of our experimental result with the available calculations (Table IV) can be made only if the Hughes-Eckhart null result for the specific mass shift of the 3^3D state is assumed. Using the results of Ref. 19, $\delta_{\text{theor}}(^3\text{He}/^4\text{He}) = 3830$ MHz; using the results of Ref. 20, $\delta_{\text{theor}}(^3\text{He}/^4\text{He}) = 3814$ MHz. Our experimental result is $\delta_{\text{exp}}(^3\text{He}/^4\text{He}) = 3805(\pm 12)$ MHz, in close agreement with the theoretical calculations.

Our experimental results can be combined with the theoretical calculations of the 2^3P state to set limits upon any possible specific mass shift of the 2^3D state.²¹ The more accurate calculation of the 2^3P state appears to be Ref. 20, where a 560-term

expansion of the wave function was employed to determine the mass polarization effect to an accuracy of one part in 10^4 . Combining this result with the normal mass shift given in Table IV we find the specific mass shift of the 3^3D state to be $9(\pm 12)$ MHz.

ACKNOWLEDGMENTS

We thank T. A. Miller for helpful discussions concerning the magnetic Hamiltonian and D. Henderson and R. H. Storz for help with the experimental apparatus.

-
- ¹L. C. Bradley and H. Kuhn, *Nature* **162**, 412 (1948); A. Andrew and W. W. Carter, *Phys. Rev.* **74**, 838 (1948); Fred, Tomkins and Brody, *ibid.* **75**, 1772 (1949).
- ²M. Fred, F. S. Tomkins, J. K. Brody, and M. Hamer-mesh, *Phys. Rev.* **82**, 406 (1951).
- ³P. F. Liao, R. R. Freeman, R. Panock, and L. M. Humphrey, *Opt. Commun.* (in press).
- ⁴M. S. Sorem and A. L. Schawlow, *Opt. Commun.* **5**, 148 (1972).
- ⁵J. E. Lawler, A. I. Ferguson, J. E. Goldsmith, D. J. Jackson, and A. L. Schawlow, *Phys. Rev. Lett.* **42**, 1046 (1979).
- ⁶W. C. Martin, *J. Phys. Chem. Ref. Data* **2**, 257 (1973). Note the substantial additions and corrections compared to ⁴He entries in C. Moore, *Atomic Energy Levels*, Nat. Stand. Ref. Data Ser. (National Bureau of Standards, Washington D.C., 1971), Vol. 1.
- ⁷J. M. Bassalo, *J. Phys. B* **9**, L181 (1976).
- ⁸Ph. Cahuzac and R. Damaschini, *Opt. Commun.* **20**, 111 (1977). Note that the reported broadening coefficient of 70 MHz/Torr by these authors was measured in the 0.1–1.0-Torr region.
- ⁹T. A. Miller and R. S. Freund, in *Advances in Magnetic Resonance*, edited by J. S. Waugh (Academic, New York, 1977), Vol. 9, p. 49.
- ¹⁰In arriving at Eq. (4) we have assumed that the anti-symmetric term involving \vec{K} in the $\vec{I} \cdot \vec{\chi}$ is much smaller than C , D , or E .
- ¹¹H. A. Bethe and E. A. Salpeter, *Quantum Mechanics of One- and Two-Electron Atoms* (Springer, Berlin, 1957).
- ¹²P. R. Bevington, *Data Reduction and Error Analysis in the Physical Sciences* (McGraw-Hill, New York, 1969).
- ¹³A. R. Edmonds, *Angular Momentum in Quantum Mechanics* (Princeton University Press, Princeton, N.J., 1960).
- ¹⁴M. Rotenberg, B. Bevens, N. Metropolis, and J. Wooten, Jr., *The 3-j and 6-j Symbols* (Technology Press, M.I.T., Cambridge, Mass., 1959).
- ¹⁵H. G. Kuhn, *Atomic Spectra* (Academic, New York, 1969).
- ¹⁶D. S. Hughes and C. Eckart, *Phys. Rev.* **36**, 694 (1930).
- ¹⁷See Ref. 15, p. 371, Eq. (57); see also Ref. 2, Section (b).
- ¹⁸A. P. Stone, *Proc. Phys. Soc. London A* **68**, 1152 (1955).
- ¹⁹M. Machacek and C. W. Scherr, *J. Chem. Phys.* **39**, 3151 (1963); M. Machacek, F. C. Sanders, and C. W. Scherr, *Phys. Rev.* **137**, A1066 (1965); *ibid.* **136**, A680 (1964). Calculations of specific mass shift on Table IV use energies of 1965 reference.
- ²⁰B. Schiff, H. Lifson, C. L. Pekeris, and P. Rabino-witz, *Phys. Rev.* **140**, A1105 (1965); *Y. Accad.*, C. L. Pekeris, B. Schiff, *Phys. Rev. A* **4**, 516 (1971).
- ²¹J. M. Burger and A. Lurio, *Phys. Rev. A* **3**, 76 (1971).